Chemical Engineering Journal 145 (2008) 86–92

Contents lists available at ScienceDirect

Chemical Engineering Journal

journal homepage: www.elsevier.com/locate/cej

Hydrogen sulphide removal from biogas by zeolite adsorption Part I. GCMC molecular simulations

Paolo Cosoli*, Marco Ferrone, Sabrina Pricl, Maurizio Fermeglia

Molecular Simulation Engineering (MOSE) Laboratory, Department of Chemical, Environmental and Raw Materials Engineering (DICAMP), University of Trieste, Piazzale Europa 1, 34127 Trieste, Italy

ARTICLE INFO

Article history:
Received 4 October 2007
Received in revised form 9 July 2008
Accepted 13 July 2008

Keywords:
Monte Carlo methods
Molecular simulation
Biogas
Hydrogen sulphide removal

ABSTRACT

In this work Grand Canonical Monte Carlo (GCMC) simulations have been used to study hydrogen sulfide (H_2S) removal from biogas streams by different zeolites such as FAU (Faujasite, NaX and NaY), LTA (zeolite A (Lynde division, Union Carbide)) and MFI (Zeolite Socony Mobil – five). Additionally, quantum mechanics (QM) molecular simulations have been performed to obtain structures and partial charges of some sorbates. The computational procedure adopted has been validated by comparison with experimental data available for H_2S removal in atmospheric environment by zeolite NaY. In order to obtain a priority list in terms of both H_2S isotherms and adsorption selectivity, adsorption simulations for pure H_2S at low pressures and for a prototype biogas mixture (i.e., CO_2, CH_4, and H_2S) have been performed and compared. The adsorption mechanisms and competition for accessible adsorption sites in terms of thermodynamic behavior have been also examined. Overall, the results obtained in this work could be routinely applied to different case studies, thus yielding deeper qualitative and quantitative insights into adsorption pollutant removal processes in environmental fields.

1. Introduction

Pollutant removal from biogas is of crucial importance to guarantee better performances in biogas exploitation processes, and to reduce environmental impact of gaseous emissions. Biogas production and utilization is constantly increasing, as it represents a "green", renewable energy, obtainable in a relatively economical way from anaerobic digestion [1–6]. Nevertheless, one of the most harmful pollutants, hydrogen sulfide (H_2S), is a biogas component, in a concentration range spanning from 10–30 to 1000–2000 ppm. Considering that exposure to a concentration of only 300 ppm for 30 min is enough to render a worker unconscious, it is clear that this fraction has to be dramatically reduced [1] to the lower toxic limit (i.e, at least 10 ppm [1,7]).

In some cases, aerobic biological processes, catalytic or oxidative processes can be used [8,9]; the use of adsorption processes, exploiting various types of adsorbents, is also widespread [10,11]. Zeolite materials are particularly suitable for adsorption removal processes [11–14], by virtue of their high selectivity and compatibility towards polar compounds, such as H_2S. Hydrophilic zeolites, with a high content of Al in their tetrahedrical framework, are generally more appropriate for polar molecules adsorption, while hydrophobic zeolites are effective in the entrapment of apolar molecules [15]. In this work we investigated the potentialities of a series of zeolites for H_2S removal, using molecular simulation techniques such as Grand Canonical Monte Carlo (GCMC) [16], and *ab initio* quantum mechanics (QM).

Molecular simulations have become a powerful tool to explore both material science and life science fields; accordingly, we believe that these techniques have reached the stage to be successfully – and intensively – employed in environmental applications, determining a gain of time, money savings and the possibility to explore applications in an easier way [17]. Thus, in what follows we employed molecular simulations for ranking a list of selected zeolites in terms of selectivity and adsorption isotherms, giving also insights on adsorption mechanisms at atomistic level from a thermodynamic point of view. Relevant experimental data are scarce [12,18], and usually given in terms of pure contaminant adsorption isotherms. Nevertheless, some studies about H_2S vapor–liquid equilibria by means of molecular simulation techniques are available [19], or about vapor–liquid coexistence of H_2S in mixtures [20], these works are based upon the Gibbs Ensemble Monte Carlo Method [21].

Thus, in order to validate the computational procedure adopted we decided to compare our calculation with experimental adsorption isotherms of pure H_2S on zeolite NaY [12], and to examine

* Corresponding author. Tel.: +39 040 558 3757; fax: +39 040 569823.
E-mail address: paolo.cosoli@dicamp.units.it (P. Cosoli).

1385-8947/$ – see front matter © 2008 Elsevier B.V. All rights reserved.
doi:10.1016/j.cej.2008.07.034

the differences encountered in a realistic situation, when a biogas mixture of CO_2, CH_4, and H_2S at low pressures is considered. Finally, isosteric heats of adsorption, total energy contributions and energy densities were the selected quantities to investigate adsorption competition at different pressures, and zeolite selectivity [22].

2. Materials and methods

Simulations were carried out on an Intel bi-processor XEON 32bit workstation. We used Sorption and *DMol³* software modules of *Materials Studio* (v. 4.0, Accelrys, San Diego, CA, USA), and in-house developed software. Stochastic methods have been described in our previous work [23] or elsewhere [24,25]; hence, here we will only briefly describe Metropolis [16] and Configurational Bias [26] methods.

Generally speaking, during a sorption simulation the chemical potential μ is kept fixed, creating a certain number of configurations of molecules to be adsorbed on a given framework. In the Grand Canonical ensemble, the chemical potentials of all components and the temperature are fixed as if the framework is in open contact with an infinite sorbate reservoir at a given temperature. The reservoir is completely described by temperature and fugacity of all components, and does not have to be simulated explicitly. Chemical potentials for each component are related to the fugacity (or partial pressure) f of the components; the reservoir, in this study, is always treated as an ideal-gas system, due to the low bulk pressures taken into account, thus, partial pressures have been considered.

Molecules can be created, translated, rotated or destroyed. Equilibrium is reached when temperature and chemical potential of the external reservoir (i.e., free gas outside the framework) and the framework are equal. The Metropolis sampling method generates chain of configurations with the ensemble probability. Transforming a configuration involves a random displacement of each atom in the system from its actual position; as in this case sorbates are flexible, trajectories are employed (see Additional Information). A trial move is accepted if it lowers the configuration energy of the system. If the configuration energy is increased, trials are accepted with a probability proportional to a Boltzmann factor: $P = e^{-\Delta U/kT}$, where ΔU is the configuration energy difference. Configurational bias (CBMC) methods are widely used to simulate adsorption of rather large and flexible molecules. In a CBMC sorption simulation, a bias is introduced towards high energy values, to avoid attempt of sampling configurations with low probabilities, which are likely to be rejected by the acceptance test [26].

In this work, adsorbed molecules are rather small if compared to all zeolite pore size; nevertheless, we decided to test both methods. Since the results for biogas adsorption isotherms in zeolites obtained with Metropolis Monte Carlo (MMC) and CBMC revealed negligible differences (see Supplementary material), we decided to adopt the MMC technique, being computationally faster than CBMC. H_2S molecular model has been built and optimized at QM density functional theory (DFT) [27] level with the *DMol³* module, due to its flexibility and dipole moment; structures of the symmetrical CH_4 and symmetrical and linear CO_2 molecules have been minimized, and partial charges assigned by the selected Force Field, the cvff_aug (consistence valence augmented forcefield).

Four zeolites were considered: LTA, FAU NaX, FAU NaY, and MFI. The first three frameworks are hydrophilic, and already employed for H_2S adsorption [12,28,29]. The last one, MFI, is hydrophobic in nature, and has been taken into account to investigate adsorption differences between these categories. 3D molecular models of LTA (Si/Al = 1), NaX (Si/Al = 1), NaY (Si/Al = 2.5) and dealuminated MFI [30] were available in the structural database of *Materials Studio*. Aluminum substitutions have been performed by following Loewenstein's rule [31], while Na^+ ions position has been assigned by in-house developed software for identifying potential energy minima and, thus, most probable extra-framework cation positions.

An all-atom model has been chosen for calculation; the *cvff_aug* was the potential energy expression of choice in all calculations [32]; a more detailed description of all molecule models is given in Additional Information. Electrostatic energy terms have been computed by the Ewald summation method. van der Waals interactions have been calculated with the classical Lennard–Jones function [33]; the cut off for van der Waals contribution, has been set to 8.5 Å, with an atom based calculations and cubic spline truncation; the cut-off distance should be less than a half of the minor cell side, so when necessary (zeolite MFI) we duplicated cells. The cubic spline truncation was set to 1 Å with a buffer of 0.5 Å; in this way, the van der Waals non-bond energy term is splined from its full value to zero within a radio of 1 Å. For electrostatic contributions, the accuracy of Ewald and group calculation was 0.001 kcal/mol with the same cut off and buffer. At least 1×10^7 productive Monte Carlo steps (i.e. Monte Carlo trial moves), preceded by 1×10^6 equilibration steps, have been performed under 3D periodic boundary conditions. Overall, we performed and compared MMC for pure H_2S adsorption (from 10 up to 1000 Pa), and competitive, simultaneous adsorption of H_2S, CH_4 and CO_2, with partial pressure in the range of a typical biogas (CO_2 and CH_4 with low concentrations of H_2S) and a bulk pressure P_{total} = 1 atm. The simulation temperature was fixed at 298 K, which is a realistic temperature for a biogas exiting from a mesophilic process [1,2,6].

Adsorption thermodynamics were further investigated analyzing the values of the isosteric heat of adsorption, Q_{RF}, which is a measure of adsorption capabilities of a sorbate in an adsorbent framework. Q_{RF} is defined as the difference between the partial molar enthalpy of the sorbate component in the external reservoir (i.e., free gas) and in the framework; accordingly, it is a measure of the enthalpy change involved in the transfer of a solute from the reference state to the adsorbed state at a constant solid phase concentration [34]:

$$Q_{RF} = h_R - h_F \quad (1)$$

Evaluation of Q_{RF} requires the application of Clausius–Clapeyron equation [34]:

$$Q_{RF} = (v_S - v_F)\left[\frac{dp}{d(\ln T)}\right] \cong RT\left[\frac{d(\ln p)}{d(\ln T)}\right] \quad (2)$$

where v_R and v_F are the sorbate partial molar volumes in the reservoir and in the framework, respectively, p the partial pressure, and T the temperature. In the right-hand side term of Eq. (2), the partial molar volume of the gas molecules in the framework is neglected with respect to that in the reservoir, and the gas behavior in the reservoir is assumed to be ideal. This leads to the expression of Q_{RF} in the Grand Canonical ensemble, where the free energy G can be calculated:

$$Q_{RF} = RT - G \quad (3)$$

A further criterion for investigating adsorption is given by the analysis of the total energy components of the system and the energy distributions. In the first case, the total energy E_M of a specific configuration of the simulation, M, is given by the Coulomb (i.e., electrostatic) and van der Waals (i.e., dispersion) contributions:

$$E_M = E_M^{SS} + E_M^{SF} + U_M^{S} \quad (4)$$

where E_M^{SS} is the intermolecular energy between the sorbate molecules, E_M^{SF} is the interaction energy between the sorbate

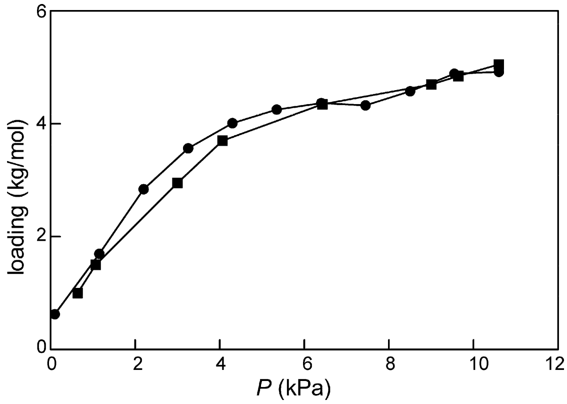

Fig. 1. Comparison between experimental adsorption isotherms [12] of H_2S on NaY (Si/Al = 2.5) (■), and GCMC calculated adsorption isotherms (●). Lines serve as eye guides.

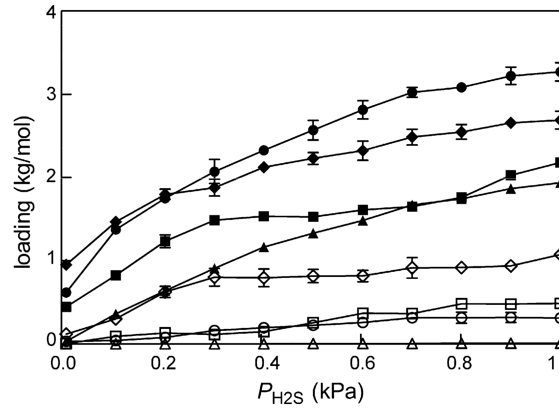

Fig. 2. Sorption isotherms for pure H_2S and H_2S in a biogas mixture. Pure H_2S simulations: (♦), NaY; (■), NaX; (●), LTA; (▲), MFI. Biogas mixture simulations: (◊), NaY; (□), NaX; (○), LTA; (△), MFI. Lines serve as eye guides.

molecules and the framework, and U_M^S is the total intramolecular energy of the sorbate molecules, as a sum of intramolecular energies of all sorbates. The intramolecular energy of the framework is not included as the framework is fixed throughout the simulation. The energy distribution curves for each sorbate express sorbate-framework interactions over the entire cell volume; in this case, the interaction energy expressions take the form of Eq. (4) with the obvious exclusion of the last term U_M^S. In the case of a mixture adsorption, the selectivity factor S_{ij} can be also considered, as given by [35,36]:

$$S_{ij} = \left(\frac{x_i}{x_j}\right)\left(\frac{y_j}{y_i}\right) \quad (5)$$

where x_i, x_j are the molar fractions of species i and j in the gas phase, while y_i and y_j are the molar fraction of species i and j adsorbed in the framework.

3. Results and discussion

Initially, we compared our simulated H_2S adsorption isotherms on zeolite NaY at 298 K with the corresponding, available experimental data [12]. As shown in Fig. 1, a good agreement is obtained. Small differences may be related, for instance, to the presence of impurities in original zeolite, and to the possibly different Si/Al ratio.

Simulation results for biogas purification are shown in Fig. 2. Considerably different behaviors for adsorption isotherms of pure

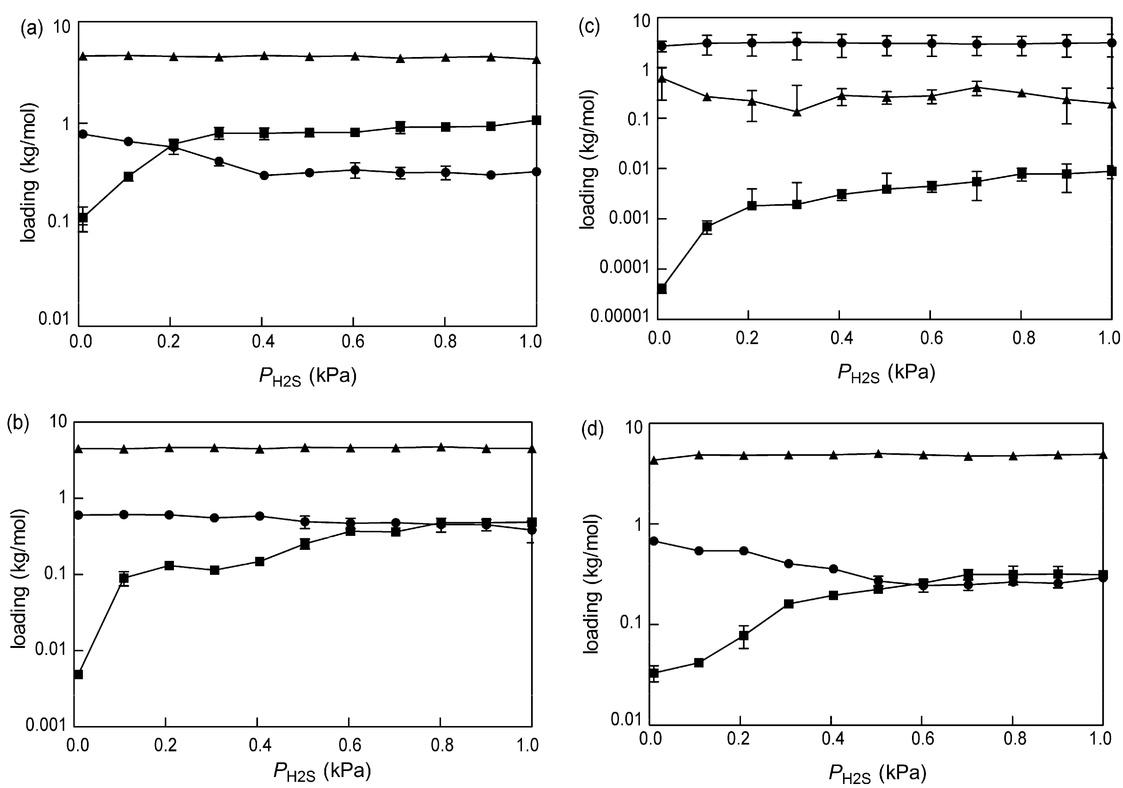

Fig. 3. H_2S, CO_2 and CH_4 adsorption isotherms as a function of H_2S partial pressure in NaY (a), NaX (b), MFI (c), and LTA (d). Symbols legend: (■), H_2S; (▲), CO_2; (●), CH_4. Lines serve as eye guides.

Table 1
Average values of Q_{RF} for a biogas mixture adsorption process, and non-bond energy components relative to adsorption at P_{H_2S} = 1000 Pa

Zeolite	Q_{RF} (kcal/mol)			Total energy contributions (P_{H_2S} = 1000 Pa) (kcal/mol)	
	H_2S	CO_2	CH_4	van der Waals	Coulomb
FAU NaY	17.9 (0.4)	11.4 (0.1)	7.2 (0.4)	−300.3 (9.4)	−502.9 (13.0)
FAU NaX	15.6 (0.6)	12.3 (0.1)	9.7 (0.1)	−302.3 (8.6)	−541.1 (14.7)
MFI	10.2 (0.4)	9.3 (0.3)	9.1 (0.2)	−179.9 (8.2)	−0.69 (0.7)
LTA	14.5 (0.2)	14.6 (0.1)	9.3 (0.1)	−389.7 (9.5)	−613.6 (13.8)

Standard deviations are reported in parenthesis.

H_2S and for the biogas mixture are obtained. These differences are qualitative, quantitative, and suggest a possible ranking of the zeolite performances. Due to the complexity of the systems and, sometimes, to the very low number of H_2S molecules adsorbed, some difficulties in Monte Carlo samplings may arise; a consequence, isotherms are not always smooth, and the error bars for each point, resulting from running multiple simulations in the same conditions, are shown to quantify the variability of the predicted values. Nevertheless, as expected, the adsorption of H_2S on the hydrophobic MFI network is always lower than all other zeolites; moreover, the considerable differences in loadings (1–4 orders of magnitude) allow a ranking among zeolites to be clearly established.

To complement the information on framework selectivity, it also instructive to examine the adsorption curves for CH_4 and CO_2 reported in Fig. 3. The isotherms of H_2S are also shown for comparison.

As expected, in hydrophilic zeolites the amount of H_2S adsorbed usually increases with increasing H_2S partial pressure; the isotherms of CH_4 slightly decrease, whilst CO_2 adsorption curves remain stable. On the other hand, when considering the apolar MFI framework, the amount of adsorbed H_2S is very low, even when considering pure component adsorption isotherms. During biogas adsorption simulations, however, the CH_4 loading remains stable, while H_2S adsorption slightly increases at the expenses of CO_2.

The global results yielded by the MMC simulations are quite sensible. In fact, electrostatic interactions between the polar molecule H_2S and the framework are more favorable in hydrophilic, ion-rich zeolites; at the same time, the increase of H_2S partial pressure is detrimental to the adsorption of the less polar molecule, CH_4. The reverse is true when considering the hydrophobic MFI framework, onto which less polar compounds are more favorably attracted, as expected. Overall, the FAU NaY zeolite seems to be characterized by the highest selectivity towards H_2S, and MFI by the lowest one. The fact that NaY could be the framework of choice, and not the NaX counterpart, in spite of the higher Si/Al ratio, could be possibly rationalized by invoking greater sterical hindrance imposed by the larger amount of sodium cations and, thus, lower pore dimensions available to H_2S binding. Analogously, the different pore shape for LTA (with the consequent confinement effects), and the different charge distribution which influence sorbate-framework interac-

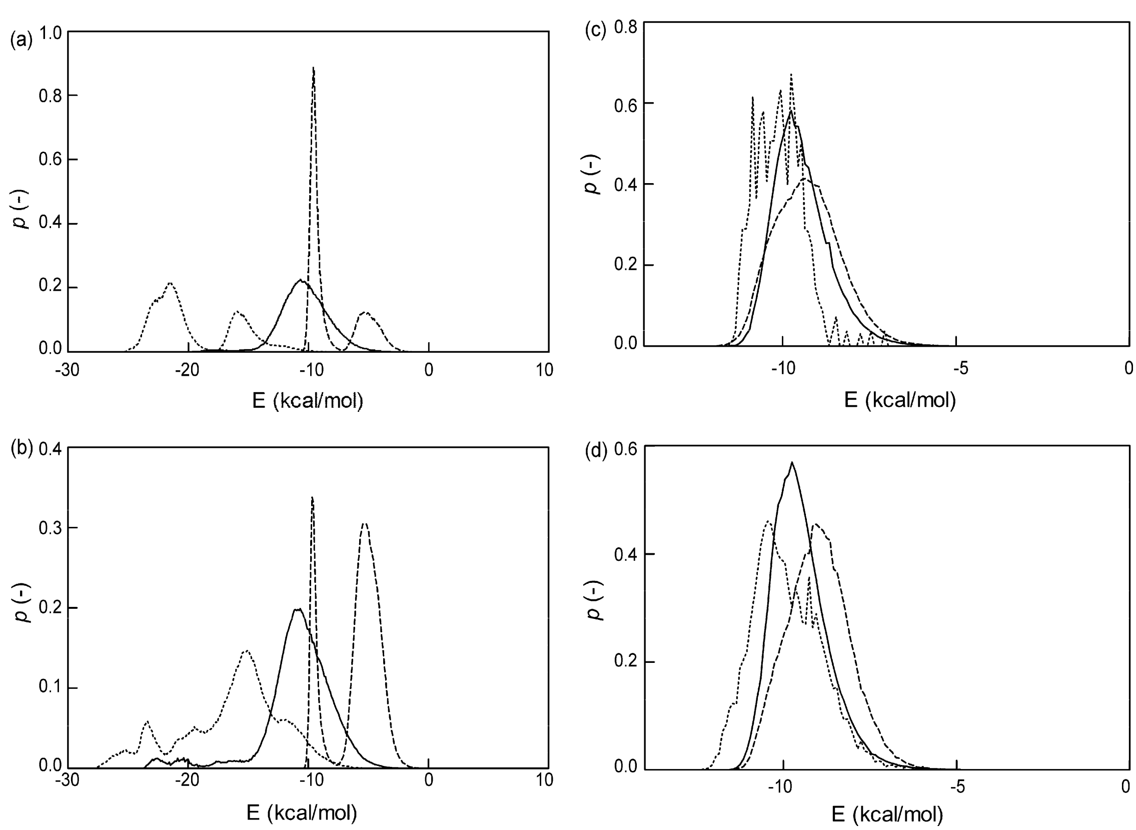

Fig. 4. Energy density distributions for biogas mixture adsorption on NaY at P_{H_2S} = 10 Pa (a), NaY at P_{H_2S} = 1000 Pa, MFI at P_{H_2S} = 10 Pa (c), and MFI at P_{H_2S} = 1000 Pa (d). Symbols legend: (······) = H_2S; (–·–·–) = CH_4; (—) = CO_2.

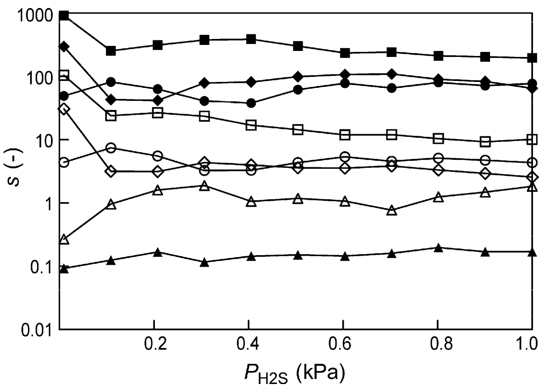

Fig. 5. Selectivity factor for H_2S with respect to CH_4 (S_{H_2S,CH_4}) (filled symbols) and to CO_2 (S_{H_2S,CO_2}) (open symbols). Symbols legend: (■, □), NaY; (●, ○), NaX; (♦, ◊), LTA; (▲, △), MFI. Lines serve as eye guides.

tions can be the main reason for the lower H_2S loading (with respect to NaX or NaY) when the mixture is taken into account.

Examining the simulation results from a thermodynamic standpoint we can confirm and further explain these tendencies. Table 1 list the calculated isosteric heats Q_{RF} for each species, averaged over different H_2S input pressures. Table 1 also reports the mean total non-bond energy components for the Metropolis Monte Carlo (MMC) sorption isotherm of the biogas mixture when $P_{H_2S} = 1000$ Pa as an example. Utterly analogous results are obtained at different H_2S partial pressures. Interestingly, the highly favorable values of the electrostatic components reveal that the different steric hindrance characterizing the three dimensional structure of the zeolite frameworks is not the only responsible for zeolite selectivity. In fact, given that the three gases do not differ very much in their molecular volumes ($V_{CO_2} = 34.0\,\text{Å}^3$, $V_{H_2S} = 30.3\,\text{Å}^3$, and $V_{CH_4} = 28.20\,\text{Å}^3$, respectively), all zeolite pore sizes are all rather large if compared to the mean radius of these molecules. Accordingly, the considered zeolites do not seem to behave predominantly as molecular sieves, but rather their selectivity appears be driven mainly by the electrostatic interactions in terms of total energy contributions.

As well evident from Table 1, Q_{RF} for H_2S is always higher than the corresponding values for CO_2 and CH_4 when the adsorption takes place on polar frameworks; interestingly, however these differences flatten for the adsorption process onto the apolar zeolite. This can be taken as a further piece of evidence that H_2S adsorption on FAU (NaY and NaX), and LTA is favored, and increases with increasing P_{H_2S}.

The density distribution profiles for the total energy confirm the same trend, as the H_2S curves show the most mean negative values in all zeolites except MFI, where this tendency is inverted. Fig. 4 illustrates this behavior in the cases of NaY and MFI at $P_{H_2S} = 10$ and 1000 Pa, respectively, as selected examples.

Fig. 4 shows different peaks for both NaY–H_2S and NaY–CH_4 energy distributions, a trend confirmed for the other hydrophilic zeolites in the entire H_2S partial pressure range. CO_2 curves, on the contrary, exhibit an invariant behavior characterized by a Gaussian distribution. As a rationale, we can say than CH_4 and H_2S are able to occupy more that one site, or position, in the framework with different probability, so that adsorption sites can be interchanged as P_{H_2S} increases. MFI curves have only one peak for each gas, and each peak is close to each other showing no appreciable differences

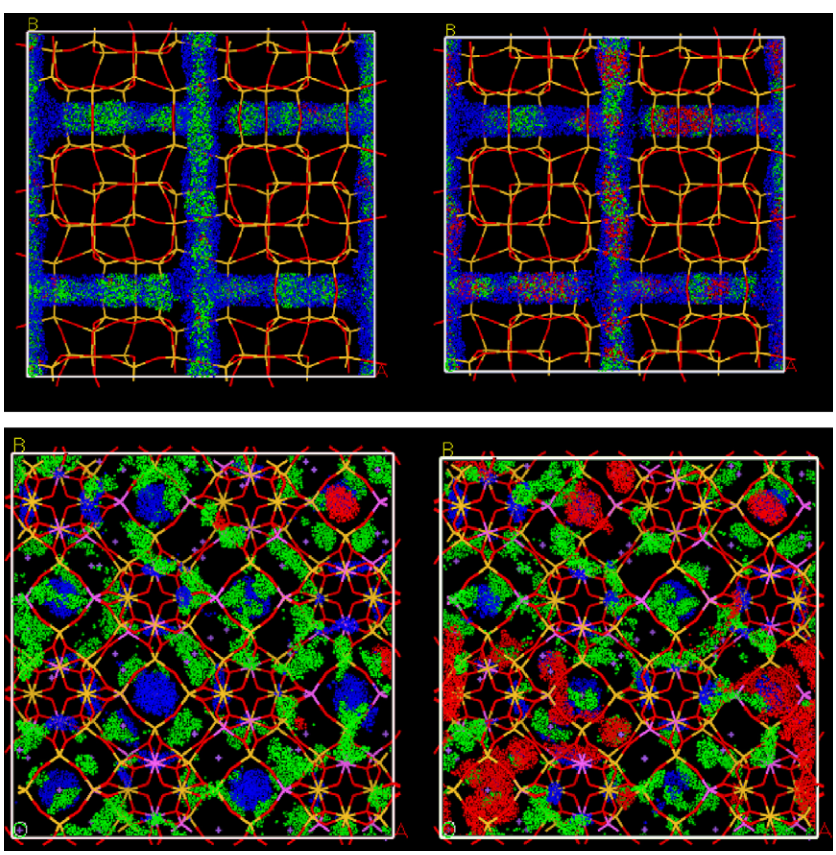

Fig. 6. Density distribution of adsorbed species in MFI (top) and NaY (bottom), $P_{H_2S} = 10$ Pa (left), and $P_{H_2S} = 1000$ Pa (right). Molecular color code: red, H_2S; blue, CH_4; green, CO_2. Density ranges between 0 and 0.3.

in E values. Accordingly, sorption site interchange is more difficult in the MFI apolar framework. To consider more details of adsorption selectivity, we mapped H_2S selectivity with respect to CH_4 and CO_2 in Fig. 5.

Selectivity factors are generally very high in hydrophilic zeolites; again, according to our simulations, the best results are achieved with NaY. To find a rationale for these selectivity curves is less straightforward. As a general observation, they tend to decrease quickly for NaY and LTA; accordingly, selectivity is generally higher at low H_2S partial pressures, which indicates that sorption selectivity mechanism seems to work better in the typical low range of biogas H_2S content. Lower selectivity for NaY and LTA may be explained by the fact that, when P_{H_2S} increases, H_2S gains new adsorption sites, for which H_2S is favored over CH_4 and CO_2, but not as well as for old adsorption sites, at lower P_{H_2S}. Selectivity for NaX shows less variation, probably because selectivity values at low H_2S pressures are already quite low. This, in turn, could be due to the higher steric hindrance exerted by the higher number of cations characterizing this framework. Once again, MFI does not show selectivity for H_2S.

We also investigated the density fields in the pores of the zeolite 3D periodic structures (Fig. 6). Although for low P_{H_2S} in some cases, distributions are not symmetrical, it is qualitatively evident how H_2S prevalently substitutes CH_4 in sorption sites (especially in larger pores). Zeolites NaX and LTA show similar behaviors, while MFI adsorption site substitutions are much less evident, if at all.

4. Conclusions

The main results of this work confirm that hydrophilic zeolites are more indicated for H_2S adsorption. Differences arise, as evidences by both pure H_2S and biogas mixture adsorption simulations, from adsorption site competition.

Adsorption isotherms, isosteric heats of adsorption and energy distributions confirm specific trends and explain adsorption behaviors. Results are of remarkable practical use if considered in terms of selectivity, according to which a ranking for the considered zeolites towards H_2S can be formulated: the FAU NaY framework appears the best choice, being favored over NaX, which has essentially the same structure but a different Si/Al ratio, ultimately resulting in more sterical hindered pores. In this way, a reasonable ranking for the best zeolite choice has been determined. It should be noticed that for some kinds of zeolites, as LTA or MFI, H_2S is scarcely adsorbed when mixture are considered, this affects the shape of adsorption isotherms and, probably, the accuracy of Monte Carlo sampling. In these cases, further analysis may be performed to obtain much quantitative results. This can be obviously done by speeding up calculations or applying new, more efficient sampling methods, which is out of the scope of the present work.

Acknowledgement

We like to acknowledge Dr. Roberto Millini for the helpful discussions and support.

Appendix A. Supplementary data

Supplementary data associated with this article can be found, in the online version, at doi:10.1016/j.cej.2008.07.034.

References

[1] U. Marchaim, Biogas Technology as an Environmental Solution to Pollution, Bull. FAO Agric. Services, Rome, Italy, 1992.
[2] R.E. Speece, Anaerobic Biotechnology for Industrial Wastewaters, Archae Press, Nashville, Tennessee, USA, 1996.
[3] G. Lettinga, A.F.M. van Velsen, S.W. Hobma, W. de Zeeuw, A. Klapwijk, Use of the upflow sludge blanket (USB) reactor concept for biological wastewater treatment, especially for anaerobic treatment, Biotech. Bioeng. 22 (1980) 699–734.
[4] A. van Haandel, M.T. Kato, P.F.F. Cavalcanti, L. Florencio, Anaerobic reactor design concepts for the treatment of domestic wastewater, Rev. Environ. Sci. Biol./Technol. 5 (2006) 21–38.
[5] K. Braber, Anaerobic digestion of municipal solid waste: a modern waste disposal option on the verge of breakthrough, Biomass Bioenergy 9 (1995) 365–376.
[6] V.N. Gunaseelan, Anaerobic digestion of biomass for methane production: a review, Biomass Bioenergy 13 (1997) 83–114.
[7] T.H. Milby, R.C. Baselt, Hydrogen sulfide poisoning: clarification of some controversial issues, Am. J. Ind. Med. 35 (1999) 192–195.
[8] S. Nishimura, M. Yoda, Removal of hydrogen sulphide from an anaerobic biogas using a bioscrubber, Water Sci. Technol. 36 (1997) 349–356.
[9] J.S. Eow, Recovery of sulfur from sour acid gas: a review of the technology, Environ. Prog. 21 (2002) 143–162.
[10] A. Bagreev, T.J. Bandosz, Study of hydrogen sulfide adsorption on activated carbons using inverse gas chromatography at infinite dilution, J. Phys. Chem. B 104 (2000) 8841–8847.
[11] X. Xiaochun, I. Novochinskii, C. Song, Low-temperature removal of H_2S by nanoporous composite of polymer-mesoporous molecular sieve MCM-41 as adsorbent for fuel cell applications, Energy Fuels 19 (2005) 2214–2215.
[12] A.J. Cruz, J. Pires, A.P. Carvalho, M. Brotas de Carvalho, Physical adsorption of H_2S related to the conservation of works of art: the role of the pore structure at low relative pressure, Adsorption 11 (2005) 569–576.
[13] C.L. Garcia, J.A. Lercher, Adsorption of H_2S on ZSM5 zeolites, J. Phys. Chem. 96 (1992) 2230–2235.
[14] S. Yasyerli, I. Ar, G. Dogu, T. Dogu, Removal of hydrogen sulfide by clinoptilolite in a fixed bed adsorber, Chem. Eng. Process. 41 (2002) 785–792.
[15] Choosing an adsorption system for VOC: carbon, zeolite or polymers? U.S. Environmental protection Agency, Clean Air Technology Center, Technical Bulletin, Research Triangle Park, North Carolina, USA, 1999.
[16] N. Metropolis, A.W. Rosenbluth, M.N. Rosenbluth, A.H. Teller, Equation of State calculations by fast computing machines, J. Chem. Phys. 21 (1953) 1087–1092.
[17] J.-C. Charpentier, The triplet "molecular processes–product–process" engineering: the future of chemical engineering? Chem. Eng. Sci. 57 (2002) 4667–4690.
[18] E.S. Kikkinides, V.I. Sikavitsas, R.T. Yang, Natural gas desulphurization by adsorption: feasibility and multiplicity of cyclic steady states, Ind. Eng. Chem. Res. 34 (1995) 255–262.
[19] W. Lin, Q. Yang, C. Zhong, Molecular simulation of vapor–liquid equilibria of toxic gases, Fluid Phase Equilib. 220 (2004) 1–6.
[20] J. Delhommelle, A. Boutin, A.H. Fuchs, Molecular simulation of vapour-liquid coexistence curves for hydrogen sulfide-alkane and carbon dioxide-alkane mixtures, Mol. Simulat. 22 (1999) 351–368.
[21] S.C. McGrother, K.E. Gubbins, Constant pressure Gibbs ensemble Monte Carlo simulations of adsorption into narrow pores, Mol. Phys. 97 (1999) 955–965.
[22] R. Millini, Application of modeling in zeolite science, Catal. Today 41 (1998) 41–51.
[23] P. Cosoli, M. Ferrone, S. Pricl, M. Fermeglia, Grand Canonical Monte Carlo simulations for VOCs adsorption in non-polar zeolites, Int. J. Environ. Technol. Manage. 7 (1/2) (2007) 228–243.
[24] S.R. Jale, M. Bülow, F.R. Fitch, N. Perelman, D. Shen, Monte Carlo simulation of sorption equilibria for nitrogen and oxygen on LiLSX zeolite, J. Phys. Chem. B 104 (2000) 5272–5280.
[25] S. Suzuki, H. Takaba, T. Yamaguchi, S. Nakao, Estimation of gas permeability of a zeolite membrane, based on a molecular simulation technique and permeation model, J. Phys. Chem. B 104 (2000) 1971–1976.
[26] J.I. Siepmann, D. Frenkel, Configurational bias Monte Carlo: a new sampling scheme for flexible chains, Mol. Phys. 75 (1992) 59–70.
[27] M. Levy, Universal variational functionals of electron densities, first-order density matrices, and natural spin-orbitals and solution of the v-representability problem, Proc. Natl. Acad. Sci. U.S.A. 76 (1979) 6062–6065.
[28] H.Y. Young, K. Yang, W.H. Young, K. Seff, Crystal structure of a hydrogen sulfide sorption complex of zeolite LTA, Zeolites 17 (1996) 495–500.
[29] F. Maugé, A. Sahibed-Dine, M. Gaillard, M. Ziolek, Modification of the acidic properties of NaY zeolite by H2S adsorption—an infrared study, J. Catal. 207 (2002) 353–360.
[30] http://www.iza-structure.org/databases/.
[31] W. Loewenstein, The distribution of aluminium in the tetrahedra of silicates and aluminates, Am. Miner. 39 (1954) 92–96.
[32] J.-R. Hill, A.R. Minihan, E. Wimmer, C.J. Adams, Framework dynamics including computer simulations of the water adsorption isotherm of zeolite Na-MAP, Phys. Chem. Chem. Phys. 2 (2000) 4255–4268.
[33] R.L. June, A.T. Bell, D.N. Theodorou, Molecular dynamics study of methane and xenon in silicalite, J. Phys. Chem. 94 (1990) 8232–8240.

[34] W. Huang, W.J. Weber Jr., Thermodynamic considerations in the sorption of organic contaminants by soils and sediments. 1. The isosteric heat approach and its application to model inorganic sorbents, Environ. Sci. Technol. 31 (1997) 3238–3243.
[35] J.-M. Leyssale, G.K. Papadopoulos, D.N. Theodorou, Sorption thermodynamics of CO_2, CH_4, and their mixtures in the ITQ-1 zeolite as revealed by molecular simulations, J. Phys. Chem. B 110 (2006) 22742–22753.
[36] D. Nicholson, K.E. Gubbins, Separation of carbon dioxide methane mixtures by adsorption: effects of geometry and energetics on selectivity, J. Chem. Phys. 104 (1996) 8126–8134.